Journal of Alloys and Compounds 509 (2011) 6252–6256

Contents lists available at ScienceDirect

Journal of Alloys and Compounds

journal homepage: www.elsevier.com/locate/jallcom

Nitrogen-doped SiO_2–HNb_3O_8 for rhodamine B photodegradation under visible light

Xiukai Li[a,b,c,*], Huiqi Pan[a,b,c], Qingsong Hu[a,b,c], Chi Zhang[a,b,c]

[a] China-Australia Joint Research Center for Functional Molecular Materials, Jiangsu University, Zhenjiang 212013, PR China
[b] Institute of Science, Jiangsu University, Zhenjiang 212013, PR China
[c] School of Chemistry and Chemical Engineering, Jiangsu University, Zhenjiang 212013, PR China

ARTICLE INFO

Article history:
Received 1 November 2010
Received in revised form 3 March 2011
Accepted 4 March 2011
Available online 11 March 2011

Keywords:
Niobic acid
Nitrogen doping
Photocatalysis
Visible light
Dye degradation

ABSTRACT

Silica-pillared and non-pillared HNb_3O_8 samples were doped with nitrogen for rhodamine B photodegradation under visible light irradiation. The results indicate that silica pillaring could have significant impacts on the photocatalytic activity of the HNb_3O_8 sample. With expanded interlayer spacing and stronger adsorption ability to dye molecules, the SiO_2 pillared and nitrogen-doped HNb_3O_8 sample performed much better than the non-pillared counterpart. The characteristics of samples were investigated by techniques such as XRD, FT-IR, UV–visible diffuse reflectance spectroscopy, SEM, and TEM. The relationships between catalyst structure and performance were discussed.

1. Introduction

Semiconductor photocatalysis for environment remediation and solar energy conversion is a topic of great interest [1–4]. Many Ti- and Nb- based metal oxides have been revealed as good UV-type photocatalysts [5–8]. In view of better utilization of solar light, extensive efforts have been devoted to fabricating visible-light-responsive photocatalysts. The mostly adopted method to modify the UV-type photocatalysts for visible light photocatalysis is cation or anion doping [9–12]. Recently, there were also reports on single phase metal oxides that are visible light active, such as Cd_2SnO_4 [13], $BiVO_4$ [14], and Ag_2ZnGeO_4 [15].

Lamellar titanates and niobates (e.g. $K_2Ti_4O_9$, HNb_3O_8) are one type of materials constructed by stacked thin sheets built up from metal–oxygen polyhedron units. From the view point of photocatalysis, such layered configuration is favorable for the separation and transportation of photogenerated electrons and holes; moreover, the material could provide more reaction active sites at the interlayer space. Previous research demonstrated that some lamellar titanates and niobates are better photocatalysts than simple TiO_2 and Nb_2O_5, and that the acid phases (H^+-exchanged ones) could show much higher photocatalytic activities than their original salt phases [16–19]. The layered configuration of lamellar solid acids enables the materials to have unique intercalation properties [19–21]. It has been demonstrated that many organic and inorganic guest species could be intercalated into the interlayer space of lamellar solid acids, and that the obtained hybrid materials could show improved thermal stability, larger pore size, and better catalytic activity [19–23]. In the case of photocatalytic water splitting, TiO_2 or silica pillared lamellar solid acids showed notably improved activities under UV or visible light irradiation [22–24]. Recently, some transition metal oxides intercalated solid acids were reported to be visible light active [25–27]. By depositing noble metals such as Pt onto the interlayer surface, the photocatalytic activities of lamellar solid acids could be notably improved [22,28]. Nitrogen doping is one technique commonly adopted to modify wide band gap materials for visible light photocatalysis [2,11]. The intercalation property of solid acid can also have profound influence on nitrogen doping. When urea was used as a nitrogen source, it was found that the intercalation of alkaline urea species not only helped to stabilize the layered structure of solid acids but also enabled easier nitrogen doping [29,30].

There have been few reports about visible light photocatalysis over pillared solid acids. HNb_3O_8 is a simple lamellar niobic acid with protonic acidity stronger than that of titanic acid. Nitrogen-doped HNb_3O_8 exhibited superior photocatalytic activity than nitrogen-doped Nb_2O_5 and KNb_3O_8 under visible light [29,30]. Thus it is very intriguing to further modify the nitrogen-doped HNb_3O_8 for better activity. In the present study, HNb_3O_8 was purposely

* Corresponding author at: Institute of Science, Jiangsu University, No. 301 Xuefu Rd., Zhenjiang 212013, PR China. Tel.: +86 511 88797815; fax: +86 511 88797815.
E-mail address: li.xiukai@gmail.com (X. Li).

0925-8388/$ – see front matter © 2011 Elsevier B.V. All rights reserved.
doi:10.1016/j.jallcom.2011.03.033

pillared with silica and then doped with nitrogen for visible light photocatalysis. The physico-chemical properties of samples and the effect of silica pillaring on the photocatalytic activity were investigated in detail.

2. Experimental

The HNb_3O_8 solid acid was prepared by reacting KNb_3O_8 with nitric acid [31,32]. KNb_3O_8 was first prepared by heating a mixture of Nb_2O_5 and K_2CO_3 in a molar ratio of 3:1 at 900 °C for 10 h. The KNb_3O_8 sample was then stirred in nitric acid (5 mol L^{-1}, 60 ml per gram of KNb_3O_8) at room temperature for 2 days for the generation of HNb_3O_8. The HNb_3O_8 sample recovered from the acid solution was washed thoroughly with distilled water and then dried at 70 °C for 12 h. The SiO_2 pillared HNb_3O_8 sample was prepared by the two-step ion-exchange method [31]; *n*-dodecylamine and tetraethyl orthosilicate (TEOS) were used as, respectively, the pre-expanding reagent and silicon source. The *n*-dodecylamine and TEOS intercalated samples were designated as C_{12}-HNb_3O_8 and TEOS-HNb_3O_8, respectively. The TEOS-HNb_3O_8 sample was calcined at 500 °C for 4 h in air for the formation of SiO_2 pillared HNb_3O_8 (designated as SiO_2–HNb_3O_8). The nitrogen doping of HNb_3O_8 and SiO_2–HNb_3O_8 was performed according to the procedure described previously [29,30], and urea was used as a nitrogen source. Taking the doping of HNb_3O_8 for an example, HNb_3O_8 (1.0 g) was finely ground with urea (2.0 g), and then this combination was heated in a covered crucible at 400 °C for 2 h. The yellow-colored product was crushed, washed well with diluted nitric acid and distilled water, and then dried at 70 °C overnight. The nitrogen-doped samples were designated as HNb_3O_8–N and SiO_2–HNb_3O_8–N, respectively.

The phase compositions of samples were identified by X-Ray Powder Diffraction (Cu K_α radiation, Bruker AXS-D8) in the 2θ range of 3–90°. The UV–visible diffuse reflectance spectra were recorded at room temperature on a Shimadzu UV-2450 UV–vis spectrometer with barium sulfate as the reference sample. Specific surface areas of samples were deduced by the BET method (N_2 adsorption) with a NOVA-2000E instrument. FT-IR spectra of the samples were collected on a Nicolet Nexus 470 FT-IR spectrophotometer at room temperature by KBr method. Morphologies of samples were characterized using a scanning electron microscope (JSM-7001F, JEOL) and a high resolution transmission electron microscope (HR JEM-2100, JEOL).

In the activity test, 0.2 g catalyst was suspended in 100 ml rhodamine B (RhB) aqueous solution (10.0 mg L^{-1}, PH value: 7) in a pyrex reactor. The suspension was stirred in the dark for about 40 min before light was turned on. A 350 W Xe-lamp (Nanshen Company, Shanghai) equipped with UV cutoff filter ($\lambda > 400$ nm) and a water filter was used as light source. The average intensity of the incident light was ca. 50.0 mW cm^{-2}. At given irradiation time intervals, 3 ml of the reaction mixture was sampled, and separated by filtration. The concentration of RhB was determined by monitoring the changes in the absorbance maximized at 554 nm.

3. Results and discussion

HNb_3O_8 is isostructural with KNb_3O_8 and is crystallized in an orthorhombic symmetry [29,33]. It has layered structure constructed of 2D $Nb_3O_8^-$ anion slices built by corner- and edge-sharing NbO_6 octahedra, the H^+ cations are located between the slices. Fig. 1 shows the XRD patterns of HNb_3O_8 and the intercalated derivatives. The 020 diffraction peak at $2\theta = 7.8°$ for HNb_3O_8 is characteristic of the layered structure, and the *d* value (ca. 11.3 Å) corresponds to the interlayer distance. Intercalation of guest components at the interlayer space notably changed the interlayer distance of HNb_3O_8. From Fig. 1b one can see that the interlayer distance d_{020} was remarkably expanded to 30.2 Å after *n*-dodecylamine intercalation. The interlayer distance d_{020} further increased to 36.8 Å after the sample was reacted with TEOS (Fig. 1c). Upon heating at 500 °C for 4 h in air, the intercalated TEOS transformed to SiO_2. As seen from Fig. 1d, the 0 2 0 diffraction peak was clearly observed for the SiO_2–HNb_3O_8 sample, signifying that the silica pillars were formed and the layered structure was well retained for the host material. In contrast, pure HNb_3O_8 is thermally unstable and usually decomposes to *R*′-Nb_2O_5 at temperatures above 200 °C [29,30]. The d_{020} value (30.2 Å) of SiO_2–HNb_3O_8 is much larger than that (11.3 Å) of non-pillared HNb_3O_8; the value is also lager than that (25.3 Å) of a silica pillared HNb_3O_8 sample prepared with *n*-decylamine as pre-expanding reagent [31], probably because of the longer chain length of *n*-dodecylamine used in this study. Taking into account the thickness of the $Nb_3O_8^-$ anion slice is 7.5 Å [31], the interlayer spacing of SiO_2–HNb_3O_8 was calculated to be 22.7 Å (30.2 Å subtract 7.5 Å), contrast to only 3.8 Å (11.3 Å subtract 7.5 Å) of HNb_3O_8. Owing to the notably expanded interlayer distance, the surface area value of SiO_2–HNb_3O_8 was as large as 220.1 $m^2\ g^{-1}$, contrasted to only 7.2 $m^2\ g^{-1}$ of the non-pillared sample.

Fig. 2 shows the FT-IR spectra of HNb_3O_8 and its intercalated derivatives. The IR absorption in the range of 400–1000 cm^{-1} is assigned to the vibration of the $Nb_3O_8^-$ host slice [31]. Absorptions in the range of 2853–2957 cm^{-1} and 1394–1507 cm^{-1} observed for C_{12}–HNb_3O_8 (Fig. 2b) and TEOS–HNb_3O_8 (Fig. 2c) are ascribed to, respectively, the C–H symmetric/asymmetric stretching and C–H bending of the intercalated organic guests [31,34]. Additional absorptions at 1077 cm^{-1} attributable to the vibration of Si–O–Si linkages [31,34] were also observed for TEOS-HNb_3O_8 (Fig. 2c) and SiO_2–HNb_3O_8 (Fig. 2d), indicating that siliceous species (TEOS or SiO_2) have successfully intercalated into the host material. The absorptions of C-H stretching and bending models were not observed for SiO_2–HNb_3O_8, signifying that the intercalated organic species were completed decomposed after the sample was heated at 500 °C for 4 h in air. The spectrum of nitrogen-doped SiO_2–HNb_3O_8 is also shown (Fig. 2e). Compared with the spectrum of undoped SiO_2–HNb_3O_8 (Fig. 2d), the IR absorption assignable to the $Nb_3O_8^-$ host slice (400–1000 cm^{-1}) is almost unchanged for

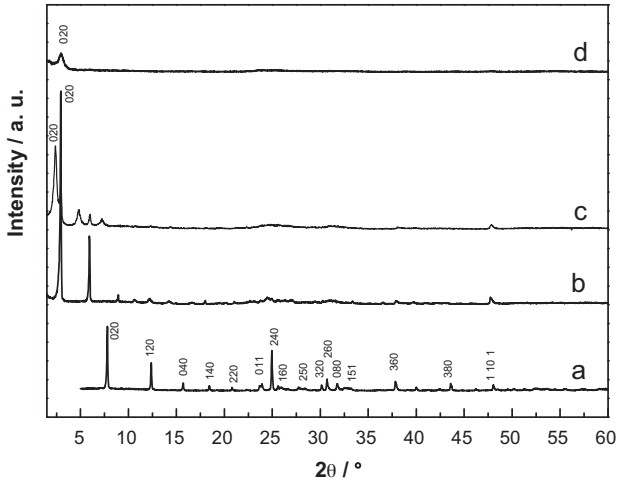

Fig. 1. XRD patterns of (a) HNb_3O_8; (b) C_{12}–HNb_3O_8; (c) TEOS–HNb_3O_8; (d) SiO_2–HNb_3O_8.

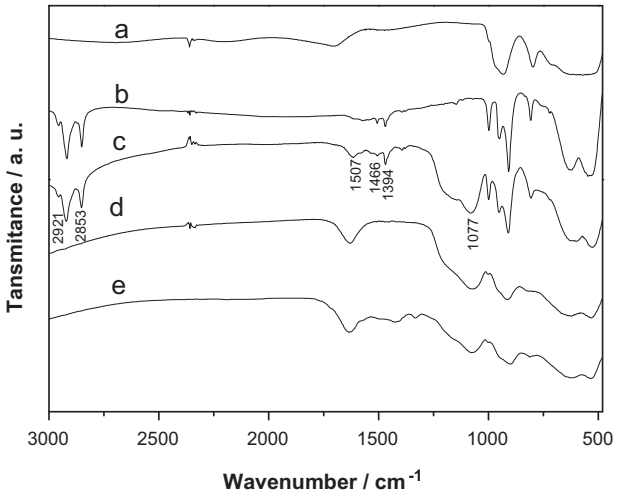

Fig. 2. FT-IR spectra of (a) HNb_3O_8; (b) C_{12}–HNb_3O_8; (c) TEOS–HNb_3O_8; (d) SiO_2–HNb_3O_8; (e) SiO_2–HNb_3O_8–N.